Organic & Biomolecular Chemistry

ROYAL SOCIETY OF CHEMISTRY

PAPER

View Article Online
View Journal | View Issue

Check for updates

Cite this: *Org. Biomol. Chem.*, 2023, **21**, 6018

Synthesis and *in vitro* photodynamic activity of aza-BODIPY-based photosensitizers†

Tamás Hlogyik,‡[a] Réka Laczkó-Rigó, ‡[b] Éva Bakos,[b] Miklós Poór,[c] Zoltán Kele,[d] Csilla Özvegy-Laczka*[b] and Erzsébet Mernyák *[a]

Received 5th May 2023,
Accepted 5th July 2023

DOI: 10.1039/d3ob00699a

rsc.li/obc

Aza-BODIPY dyes have recently come to attention owing to their excellent chemical and photophysical properties. In particular, their absorption and emission maxima can efficiently be shifted to the red or even to the NIR spectral region. On this basis, aza-BODIPY derivatives are widely investigated as fluorescent probes or phototherapeutic agents. Here we report the synthesis of a set of novel aza-BODIPY derivatives as potential photosensitizers for use in photodynamic therapy. Triazolyl derivatives were obtained *via* Cu(I)-catalyzed azide–alkyne cycloaddition as the key step. *In vitro* photodynamic activities of the newly synthesized compounds were evaluated on the A431 human epidermoid carcinoma cell line. Structural differences influenced the light-induced toxicity of the test compounds markedly. Compared to the initial tetraphenyl aza-BODIPY derivative, the compound bearing two hydrophilic triethylene glycol side chains showed substantial, more than 250-fold, photodynamic activity with no dark toxicity. Our newly synthesized aza-BODIPY derivative, acting in the nanomolar range, might serve as a promising candidate for the design of more active and selective photosensitizers.

1. Introduction

Organic fluorophores are utilized in several bioapplications; however, they must meet numerous requirements, including easy availability, strong absorption, preferably in the near-infrared region (NIR), and tunable photophysical properties.[1–4] Nowadays, rhodamine, cyanine, and boron-dipyrromethene (BODIPY) dyes are the most commonly used organic compounds for bioapplications. Nevertheless, all of them possess several drawbacks, such as limited synthetic availability, low fluorescence quantum yields, and low emission maxima or optical instability. BODIPY dyes stand out with their excellent photophysical properties and post-functionalization capabilities. However, their low absorption maxima limit their applications, especially, when a higher penetration depth is required.[5] The favorable properties of BODIPY dyes are retained in their aza counterparts, which are formally available upon replacing the C-8 atom with a nitrogen atom.[5,6] Additionally, the absorption and emission maxima of the latter are highly improved, reaching the red or even the NIR region. Owing to their excellent chemical and photophysical properties, aza-BODIPY dyes have recently come to attention. They have been widely investigated not only as fluorescent probes[7] but also as promising phototherapeutic agents.[8] Special attention has recently been paid to utilize aza-BODIPY dyes as potential photosensitizers in photodynamic therapy (PDT).[6] PDT is a minimally invasive approach for cancer therapy and other medical purposes.[1] The basis of PDT is the photoexcitation of a photosensitizer (PS) that produces cytotoxic reactive oxygen species, which then induce various cellular processes finally leading to cell death. On the other hand, ideally, the photosensitizer should have no dark toxicity allowing specific treatment by focused illumination of the targeted tissue. The first aza-BODIPY-based photosensitizers were prepared by O'Shea and colleagues in 2002.[6] Later, singlet oxygen yields were improved by the introduction of bromine or iodine atoms into certain positions of the dye core.[9] An important correlation appeared between the position of the halogen and fluorescence quantum yields obtained.[10–13] Heavy-atom substitutions at the pyrrole rings seemed to be more advantageous than those at the peripheral aryl rings. **PS1**, synthesized by Gallagher and O'Shea *et al.*, was proved to be an exciting PS through Phase 1 clinical trials in tumor models (Fig. 1).[14] It was shown that the direct bromo substitution on the

[a]*Department of Inorganic, Organic and Analytical Chemistry, University of Szeged, Dóm tér 8, H-6720 Szeged, Hungary. E-mail: bobe@chem.u-szeged.hu; Fax: +36 62 544200; Tel: +36 62 544277*
[b]*Drug resistance research group, Institute of Enzymology, Research Centre for Natural Sciences, Magyar tudósok körútja 2, H-1117 Budapest, Hungary*
[c]*Department of Pharmacology, Faculty of Pharmacy, University of Pécs, Rókus u. 2, H-7624 Pécs, Hungary. E-mail: laczka.csilla@ttk.hu; Tel: +3613826789*
[d]*Department of Medicinal Chemistry, University of Szeged, Dóm tér 8, H-6720 Szeged, Hungary*

†Electronic supplementary information (ESI) available. See DOI: https://doi.org/10.1039/d3ob00699a

‡These authors contributed equally to this work.

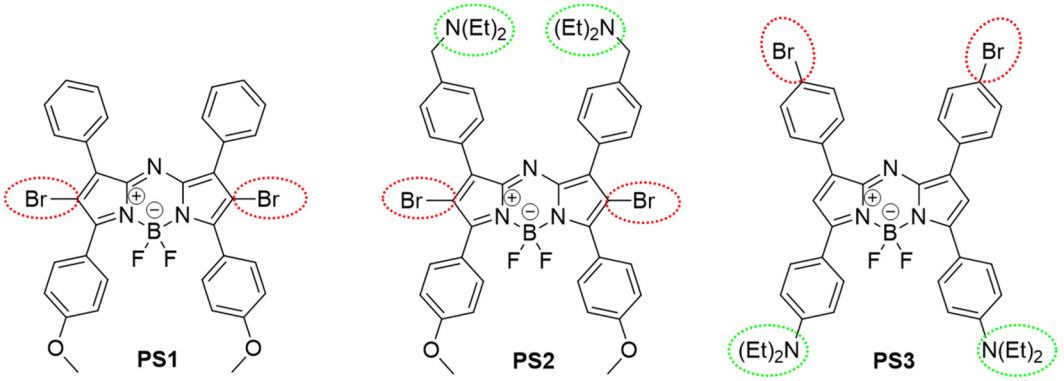

Fig. 1 Structures of aza-BODIPY-based effective PSs.

aza-BODIPY core results in efficient $^1O_2$ generation. Nevertheless, the optically beneficial heavy-atom effect often results in marked dark cytotoxicity of photosensitizers.[15–17] In spite of the several advantages of PDT in clinical treatment, its low selectivity often limits its application.[18] A PS which could be activated by tumor-associated stimuli (activatable PS: aPS) could serve as a better alternative.[19,20] O'Shea *et al.* reported recently an aza-BODIPY-based aPS (**PS2**) bearing a pH-responsive amine receptor. The utilization of **PS2** resulted in reversible off/on switching of $^1O_2$ production.[21] An acid-enhanced $^1O_2$ rate for **PS2** was determined compared to a non-acidic solution. Unwanted side effects might additionally arise from non-selective PS accumulation in both tumorous and adjacent healthy tissues.[19] The encapsulation of PSs in ligand-modified liposomes is a powerful method to improve selectivity.[22] Ju *et al.* designed a trifunctional aza-BODIPY-based aPS (**PS3**) to elaborate the selective tumor imaging methodology.[23] The presence of diethylaminophenyl groups facilitated pH-activatable $^1O_2$ generation. Encapsulation into cyclic RGD peptide-poly(ethylene glycol)-*block*-poly(lactic acid) nanomicelles enabled the formation of water-soluble nanoparticles. The self-monitoring capability of the nanoparticles provided a possibility for tracking PDT efficacy.

The introduction of hydrophilic groups into a photosensitizer might provide more favorable bioapplications due to improvements in its water-solubility and biocompatibility. One of the reported strategies includes the introduction of oligo (ethylene glycol) side chains onto the dye core.[24] Additionally, the presence of a triazole ring in biologically active compounds might also lead to the improvement of their activity, in particular, concerning anticancer agents.[25] Although certain aza-BODIPY derivatives have even reached clinical trials,[14] it is highly desired to permanently search for new candidates with improved selectivity and efficacy.

Encouraged by the predominant importance of aza-BODIPY dyes in PDT, here we aimed to synthesize new, heavy-atom-free derivatives as potential photosensitizers. The introduction of (*N*-benzyltriazolyl) or azido(triethylene glycol) side chains was planned *via* post-functionalization, utilizing the Cu(I)-catalyzed azide–alkyne cycloaddition reaction (CuAAC) as a key step. The evaluation of *in vitro* phototoxic activities of the newly synthesized dyes in A431 cancer cells was also conducted.

2. Results and discussion

2.1. Synthesis of aza-BODIPY derivatives

Aza-BODIPY derivatives might be available *via* different protocols.[26,27] Here we have selected a routine methodology starting with the Michael addition of nitromethane to chalcones (**4** and **5**) (Scheme 1). Two diaryl-α,β-unsaturated ketones (**4** and **5**), differing in the substitution pattern of the phenyl ring of the aldehyde, were synthesized *via* aldol condensation between benzaldehyde or its 4-propargyloxy counterpart and acetophenone. The addition of nitromethane afforded compounds **6** and **7** in high yields. The aza-bridge was established using ammonium acetate as the ammonia source in ethanol solvent under reflux conditions. The applied aza-BODIPY synthesis strategy is formally considered to be dimerization, and thus aryl substituents at positions C-1 and C-7 or C-3 and C-5 are identical in pairs. The azadipyrromethenes (**8** and **9**) formed were subjected to chelation with $BF_3{\cdot}OEt_2$ using triethylamine (TEA), a weak organic base, at room temperature. The establishment of the fused three-ring system is crucial in order to inhibit the rotation around the aza-bridging bonds and to obtain a fluorescent compound. Tetraphenyl derivative **10** was synthesized with the aim of getting a reference PS for biological testing. However, bis-propargyl derivative **11** allowed post-functionalization leading to potentially more promising PSs. In an effort to obtain aza-BODIPY derivatives with high photodynamic activity, compound **11** was subjected to the CuAAC reaction with two different azides as coupling partners. In the first reaction, benzyl azide was chosen as the coupling partner. The click reaction was efficiently achieved *via* our recently developed, well-established methodology, using CuI as a catalyst and PPh_3 as an accelerating ligand.[25] The (*N*-benzyltriazolyl)methyloxy compound (**15**) was obtained in an excellent yield. Our next click strategy included the introduction of hydrophilic oligo(ethylene glycol) side chains *via*

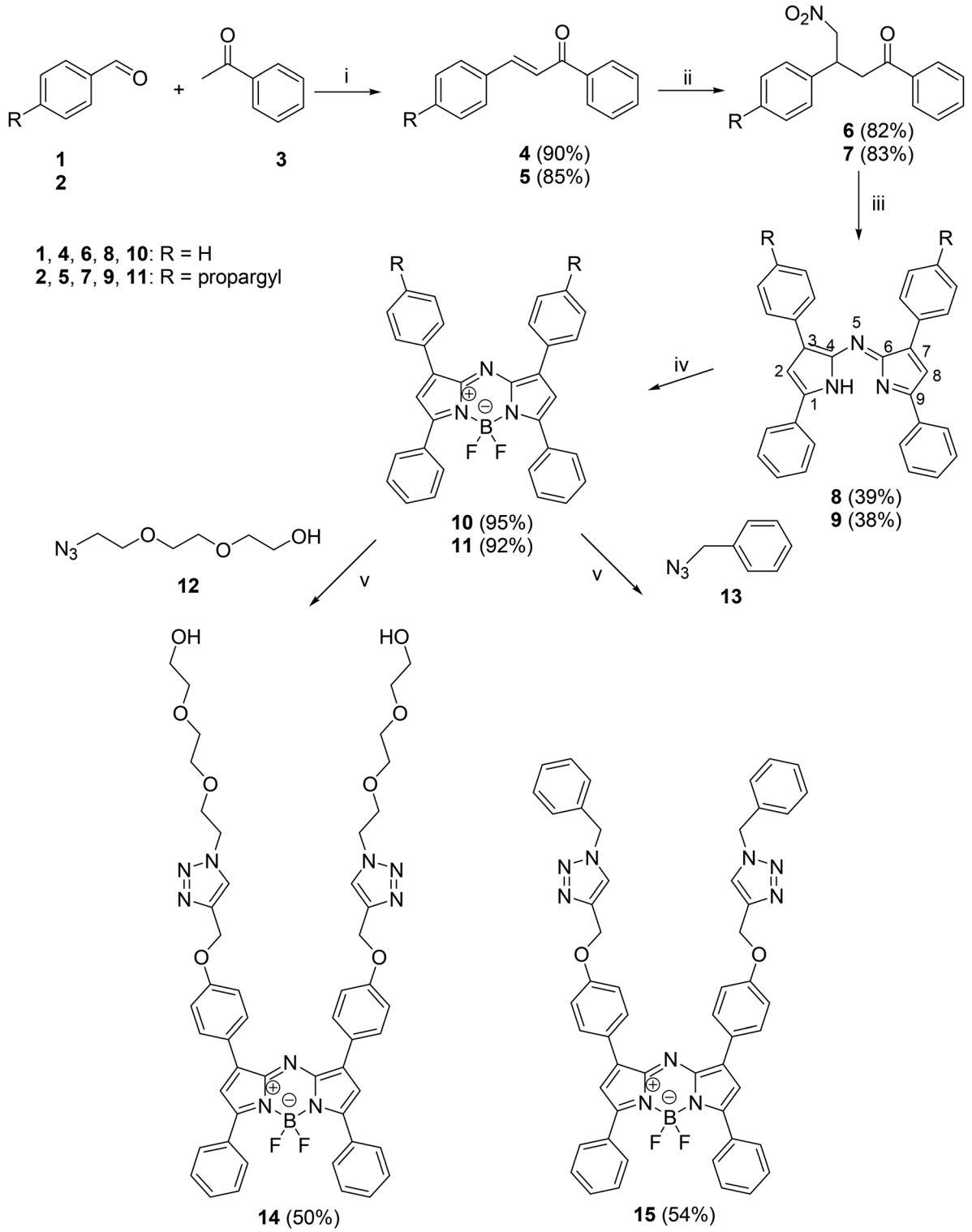

Scheme 1 Reagents and conditions: (i) NaOH (2 equiv.), methanol, rt, 2 h; (ii) catalytic amount of NaOH (0.2 equiv.), methanol, nitromethane (5 equiv.), 60 °C, 3 h; (iii) NH_4OAc (35 equiv.), ethanol, reflux, 24 h; (iv) Et_3N (10 equiv.), toluene, rt, 15 min, $BF_3{\cdot}OEt_2$ (15 equiv.), reflux, 5 h; (v) toluene, catalytic amounts of PPh_3 and CuI, 2 equiv. of **12**, 8 equiv. of DIPEA, reflux, 2 h; (vi) toluene, catalytic amounts of PPh_3 and CuI, 2 equiv. of **13**, 8 equiv. of DIPEA, reflux, 5 h.

the CuAAC reaction. Propargyl derivative **11** as a terminal alkyne was reacted with azido-triethylene glycol as an azide partner under the reaction conditions described above. The newly synthesized aza-BODIPY derivative **14**, bearing two hydrophilic side chains, might possess improved biological activity in comparison with its counterpart **11**.

2.2. Photophysical characterization of aza-BODIPY dyes

Due to their good solubility in DMF, UV-Vis and fluorescence spectroscopic properties of compounds **10**, **11**, **14**, and **15** were examined in this solvent. Among the four derivatives examined, compound **10** had the highest absorption signal, showing its maximum at 654 nm (Fig. 2A). The absorption maxima of derivatives **11**, **14**, and **15** appeared at higher wave-

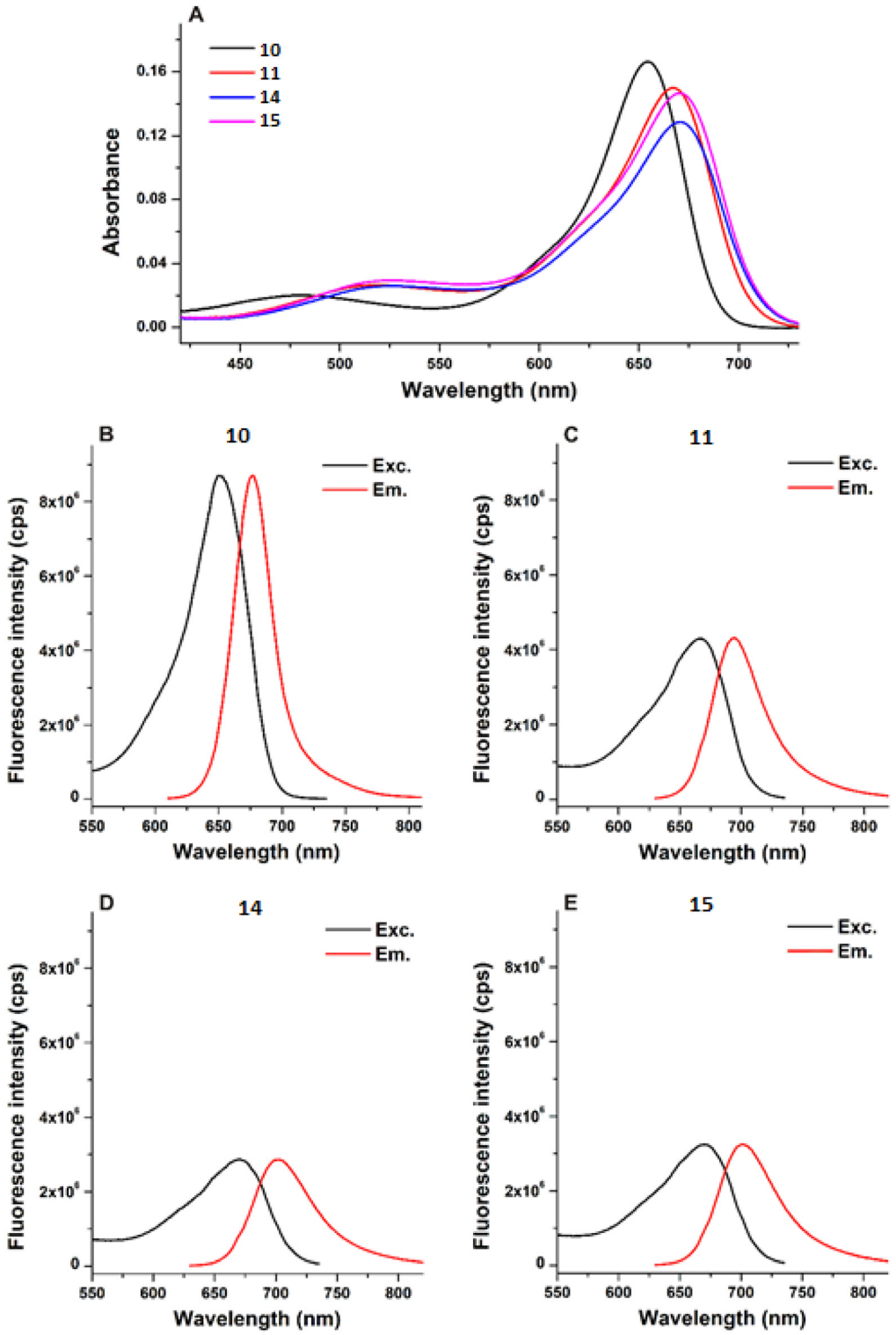

Fig. 2 Absorption spectra of compounds **10**, **11**, **14**, and **15** (A). Fluorescence excitation and emission spectra of **10** (B), **11** (C), **14** (D), and **15** (E). The representative spectra of test compounds (2 μM each) shown here were recorded in DMF at room temperature (see excitation and emission wavelengths collected in Table 1).

lengths, from 667 to 670 nm (Table 1), with the lowest absorbance observed for dye **14** (Fig. 2A). The emission wavelength maxima of the four compounds tested were between 676 and 701 nm (Table 1). Compound **10** showed the highest fluorescence emission signal (Fig. 2B), which was more than two-fold larger than those of the other three derivatives (Fig. 2C and D). It was followed by **11**, then by **15** and **14**.

2.3. Evaluation of *in vitro* dark- and light-induced toxicity of aza-BODIPY dyes

To evaluate the potential dark- and light-induced toxic effects of the aza-BODIPY dyes (**10**, **11**, **14**, and **15**), the epidermoid carcinoma cell line A431, a typical model in toxicology and cancer research, was chosen. A431 cells were incubated with increasing concentrations of the compounds for 24 hours. The next day, the compounds were removed and the cells were illuminated with an LED source of 658 nm for 10 min. Cell viability after 48 hours was determined with PrestoBlue. Dark controls were treated the same way, with the exception that they were kept in the dark throughout the experiment. Fig. 3A shows that all the compounds (**10**, **11**, **14**, and **15**) exerted only negligible dark toxicity even at 10 μM. Encouraged by the low dark toxicity results, the *in vitro* photodynamic activity of the compounds was investigated. Fig. 3B shows that compound **15** exhibited only moderate toxicity even at 10 μM. Dye **11** was found to be more active, resulting in 50% cell death already at 5 μM test concentration. Still, since compounds effective in nanomolar concentration were looked for, neither compound **15** nor compound **11** was selected for further experiments.

The two triazolyl aza-BODIPY derivatives, namely tetraphenyl compound **10** (IC_{50}: 0.96 μM) and its *bis*-triazolyl-TEG counterpart **14** (IC_{50}: 3.66 nM), resulted in efficient cell killing when irradiated, with the latter being 268-fold more active (Fig. 4). The significant increase in the phototoxicity results obtained for compound **14** might be assigned to its hydrophilic side chains present at the two phenyl rings possibly resulting in increased membrane permeability. It should be highlighted that structural differences influenced the light-induced toxicity of the test compounds markedly. The test compounds differ only in the *para*-substituents of the phenyl rings originating from the benzaldehyde starting compound or introduced by post-functionalization. To the best of our knowledge, there are no literature reports for aza-BODIPY derivatives acting on the A431 cell line in such a low nanomolar range.

Table 1 UV-Vis and fluorescence spectroscopic properties of compounds **10**, **11**, **14**, and **15** (λ_{abs}, absorption wavelength maximum; λ_{em}, fluorescence emission wavelength maximum; $\Delta\lambda$, stokes shift; ε_{max}, maximum molar absorptivity)

Compound	**10**	**11**	**14**	**15**
Solvent	DMF	DMF	DMF	DMF
λ_{abs} [nm]	654	667	670	670
λ_{em} [nm]	676	693	701	701
$\Delta\lambda$ [nm]	22	26	31	31
ε_{max} [M^{-1} cm^{-1}] (±SD)	81 987 (±7394)	74 435 (±4023)	64 505 (±5206)	73 825 (±5586)

2.4. Evaluation of *in vitro* ROS generation

Next, we investigated the mechanism of light-induced toxicity. To this aim, ROS generation by the compounds after illumination was measured using the DCF-DA dye. DCF-DA enters the cells passively, where it is converted to non-fluorescent H2-DCF by esterases. H2-DCF is then oxidized by ROS to fluorescent DCF. Fig. 5 shows that, in harmony with their phototoxicity, **10** and **14** resulted in increased ROS levels, while in cells incubated with non-toxic **11** and **15**, we observed only a small increase in ROS levels compared to the cells illuminated in the absence of the dyes.

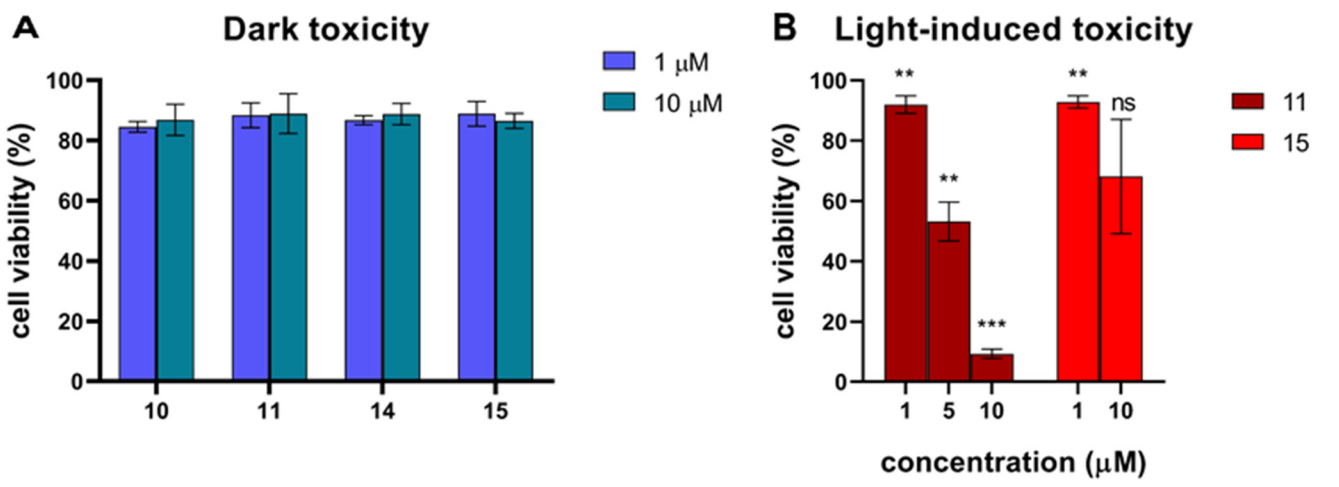

Fig. 3 (A) Dark toxicity of the test compounds (**10**, **11**, **14** and **15**) toward A431 cells at 1 μM and 10 μM test concentrations. (B) Light-induced toxicity of compounds **11** (at 1 μM, 5 μM and 10 μM) and **15** (at 1 μM and 10 μM) after illumination with an LED source of 658 nm for 10 min. The figure shows average ± SD values obtained in three biological replicates.

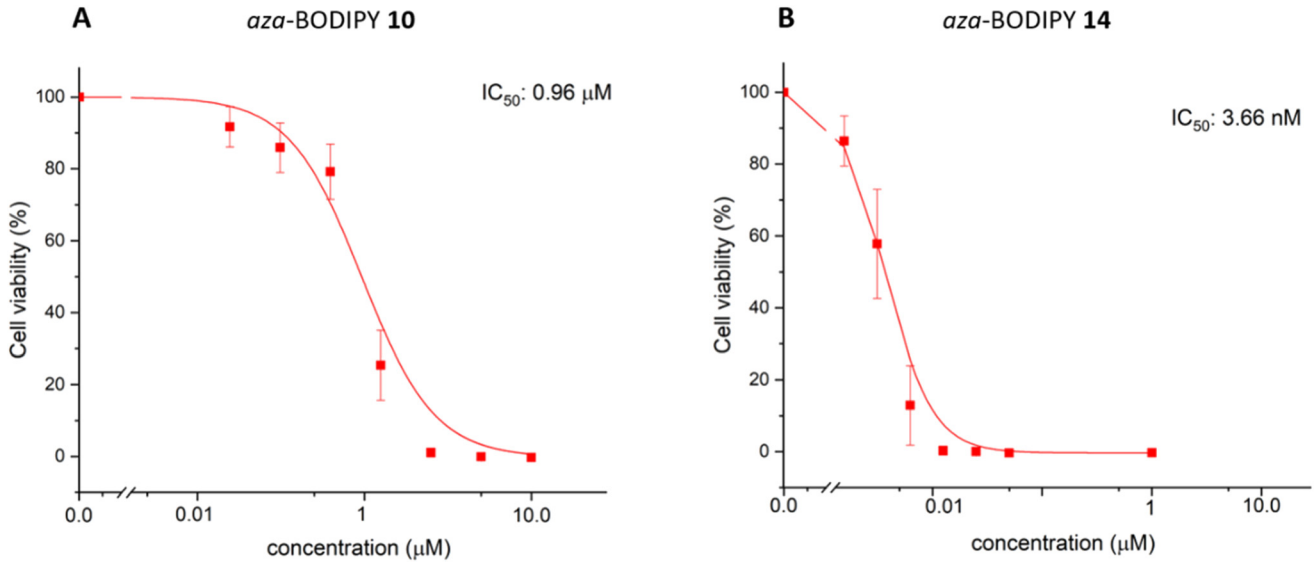

Fig. 4 Concentration-dependent light-induced toxicity of compounds **10** (A) and **14** (B) with calculated IC_{50} values.

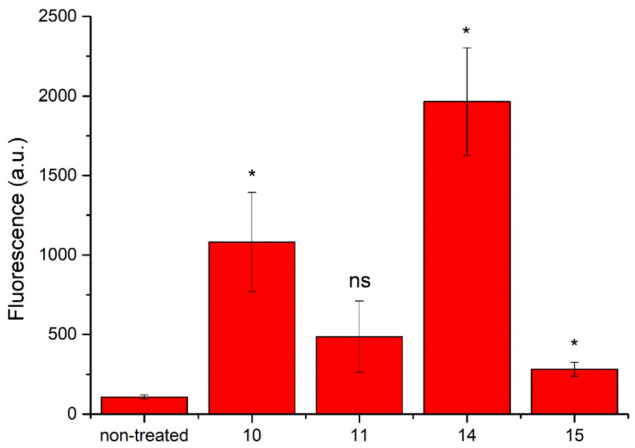

Fig. 5 Light-induced ROS generation by aza-BODIPY derivatives. A431 cells were incubated with compounds **10** (1 μM), **11** (10 μM), **14** (1 μM), and **15** (10 μM) for 24 hours. After 10 min of illumination at 658 nm, fluorescence of DCF was measured at 485/530 nm. The figure shows average ± SD values obtained in three biological replicates.

3. Conclusions

New red-emitting aza-BODIPY derivatives (**11**, **14** and **15**) were synthesized. A bis-propargyl tetraphenyl derivative (**11**) served as a terminal alkyne in CuAAC reactions with two different azide partners. The introduction of a triazole moiety was performed with the aim of increasing the anticancer potential of the compounds. The bis-triazolyl-TEG derivative (**14**) exhibited outstanding light-induced toxicity against the A431 carcinoma cell line with an excellent photo-to-dark toxicity ratio. We confirmed that post-functionalization of the tetraphenyl aza-BODIPY core might lead to superior photosensitizers without the need for the introduction of halogen atoms. The significance of our work lies in the simplicity and high efficiency of the newly synthesized compounds. Compound **14**, acting in the nanomolar range, might serve as a promising candidate for the design of more active and selective photosensitizers.

4. Experimental part

4.1. Chemistry

Melting points (Mp) were determined with Kofler hot-stage apparatus and are uncorrected. Elemental analyses were performed with a PerkinElmer CHN analyzer model. Thin-layer chromatography was performed on silica gel 60 F254 (layer thickness 0.2 mm, Merck); eluents: a: 30% ethyl acetate/70% hexanes, b: 25% ethyl acetate/75% hexanes, c: 50% dichloromethane/50% hexanes, d: 60% dichloromethane/40% hexanes, e: 10% methanol/90% dichloromethane, and f: 5% methanol/95% dichloromethane. The spots were detected with I_2 or UV (365 nm) after spraying with 5% phosphomolybdic acid in 50% aqueous phosphoric acid and heating at 100–120 °C for 10 min. Flash chromatography was performed on silica gel 60, 40–63 μm (Merck). ^{1}H NMR spectra were recorded in DMSO-d_6 or $CDCl_3$ solution with a Bruker DRX-500 instrument at 500 MHz. ^{13}C NMR spectra were recorded with the same instrument at 125 MHz under the same conditions. Mass spectrometry: full scan mass spectra of the newly synthesized compounds were acquired in the range of 100 to 1100 m/z with a Q Exactive Plus quadrupole-orbitrap mass spectrometer (Thermo Fisher Scientific, Waltham, MA, USA) equipped with a heated electrospray (HESI). Analyses were performed in positive ion mode by flow injection mass spectrometry with a mobile phase of 50% aqueous acetonitrile containing 0.1 v/v% formic acid (0.3 ml min^{-1} flow rate). Aliquots of 5 μl of samples were injected into the flow. The ESI capillary was adjusted to 3.5 kV and N_2 was used as a nebulizer gas.

4.1.2. Synthesis protocols

*4.1.2.1. Synthesis of chalcones **4** and **5**.* Benzaldehyde (**1**, 1.06 g, 10 mmol) or 4-(prop-2-ynyloxy)benzaldehyde **2** (1.60 g, 10 mmol) was dissolved in a solution of sodium hydroxide (0.80 g, 20 mmol) in methanol (10 mL), and stirred at rt for 10 minutes. Acetophenone (**3**, 1.17 mL, 10 mmol) was added, and the stirring was continued at rt for 2 h. The solvent was removed under reduced pressure, and the residue was extracted with dichloromethane (3 × 15 mL). The combined organic layers were dried over sodium sulfate and the solvent was removed under reduced pressure. Compound **4** or **5** was obtained as a yellow solid (**4**: 1.87 g, 90%; **5**: 2.28 g, 85%).

4: Mp = 55.0–57.0 °C, R_f = 0.64[a]. Compound **4** was identical to the compound described in the literature.[28,29]

5: Mp = 60.3–62.1 °C, R_f = 0.60[b]. Compound **5** was identical to the compound described in the literature.[30,31]

*4.1.2.2. Synthesis of 4-nitro-1,3-diphenylbutan-1-one (**6**) or 4-nitro-1-phenyl-3-(4-prop-2-ynyloxy-phenyl)butan-1-one (**7**).* Chalcone **4** (1.50 g, 7.2 mmol) or **5** (1.89 g, 7.2 mmol) was dissolved in a solution of 0.2 equiv. of sodium hydroxide (58 mg, 1.44 mmol) in methanol (12 mL). This was followed by the addition of nitromethane (1.92 mL, 36 mmol) and the solution was stirred at 60 °C for 3 h. The solvent was removed under reduced pressure, and the residue was extracted with ethyl acetate (3 × 15 mL) and washed with brine (1 × 10 mL). The combined organic layers were dried over sodium sulfate, and the solvent was removed under reduced pressure. Compound **6** was obtained as a pale yellow solid (1.59 g, 82%) and compound **7** as a pale yellow oil (1.93 g, 83%).

6: Mp = 68.5–69.4 °C, R_f = 0.55[a]. Compound **6** was identical to the compound described in the literature.[32]

7: oil, R_f = 0.50[a]. ESI-HRMS: *m*/*z*: 346.10547 $[M + Na]^+$ ($C_{19}H_{17}NO_4$ + Na^+ requires 346.10498 $[M + Na]^+$). ^{1}H NMR (500 MHz, DMSO-d_6) δ 3.45–3.57 (overlapping multiplets, 3H, CH_2 and C≡CH), 4.01 (m, 1H), 4.75 (d, J = 4.7 Hz, 2H, O–CH_2), 4.82 (dd, 1H, J = 12.8 Hz, J = 5.7 Hz, 1H), 4.95 (dd, 1H, J = 12.8 Hz, J = 9.7 Hz, 1H), 6.92 (d, J = 7.3 Hz, 2H), 7.31 (d, J = 7.3 Hz, 2H), 7.51 (t, J = 7.6 Hz, 2H), 7.63 (t, J = 7.6 Hz, 1H), 7.93 (d, J = 7.6 Hz, 2H). ^{13}C NMR (125 MHz, DMSO-d_6) δ 197.4 (C=O), 156.2 (C), 136.3 (C), 133.3 (CH), 132.4 (C), 128.7 (2 × CH), 128.6 (2 × CH), 127.8 (2 × CH), 114.6 (2 × CH), 79.7 and 79.2 and 78.0 (CH_2 and C≡CH), 55.2 (CH_2), 41.2 (CH_2), 38.4 (CH).

*4.1.2.3. Synthesis of (3,5-diphenyl-1H-pyrrol-2-yl)-(3,5-diphenyl-pyrrol-2-ylidene)amine **8** and 5-phenyl-3–4-prop-2-ynyloxy-phenyl-1H-pyrrol-2-yl-[5-phenyl-3-(4-prop-2-ynyloxy-phenyl)-pyrrol-2-ylidene]-amine **9**.* To a solution of compound **6** (1.20 g, 4.5 mmol) or compound **7** (1.45 g, 4.5 mmol) in ethanol (20 mL), ammonium acetate (12.1 g, 158 mmol) was added. The solution was stirred under reflux for 24 h, then cooled to room temperature and three-quarters of the solvent was removed under reduced pressure. The residue was filtered and washed with cold ethanol. The remaining solid was suspended in water and then extracted with dichloromethane (3 × 20 mL). The combined organic layers were dried over sodium sulfate and the solvent was removed under reduced pressure. The residue was purified by flash chromatography with CH_2Cl_2/hexane = 40/60 as an eluent. Compound **8** was obtained as a dark blue solid, and compound **9** as a dark green solid (390 mg, 39% for compound **8** and 475 mg, 38% for compound **9**).

8: Mp = 287.3–290.8 °C, R_f = 0.65[c]. Compound **8** was identical to the compound described in the literature.[32]

9: Mp = 234.8–236.4 °C, R_f = 0.38[c]. ESI-HRMS: *m*/*z*: 558.21836 $[M + H]^+$ ($C_{38}H_{27}N_3O_2$ + H^+ requires 558.21761 $[M + H]^+$). ^{1}H NMR (500 MHz, DMSO-d_6) δ 3.61 (s, 2H, C≡CH), 4.91 (d, J = 2.1 Hz, 2 × OCH_2), 7.12 (d, J = 7.1 Hz, 4H), 7.54 (t, J = 7.5 Hz, 2H), 7.58 (s, 2H), 7.62 (t, J = 7.5 Hz, 4H), 8.07 (overlapping multiplets, 8H). ^{13}C NMR (125 MHz, DMSO-d_6) δ 157.3 (2 × C), 154.9 (2 × C), 148.7 (2 × C), 141.2 (2 × C), 131.3 (2 × C), 130.4 (2 × CH), 129.8 (4 × CH), 129.3 (4 × CH), 126.5 (4 × CH), 126.4 (2 × C), 114.8 (4 × CH), 114.6 (2 × CH), 79.1 and 78.2 (2 × C≡CH), 55.4 (2 × OCH_2).

*4.1.2.4. Synthesis of aza-BODIPY **10** and **11**.* A stirred solution of compound **8** (314 mg, 0.69 mmol) or **9** (385 mg, 0.69 mmol) in toluene (10 mL) was treated with triethylamine (0.96 mL, 10 equiv.). The solution was stirred at rt for 15 min, then BF_3·OEt_2 (1.28 mL, 15 equiv.) was added dropwise and the solution was stirred under reflux for 5 h. After cooling to rt, the reaction was quenched using water (30 mL) and extracted with toluene (3 × 20 mL). The combined organic layers were dried over sodium sulfate and the solvent was removed under reduced pressure. The residue was purified by flash chromatography with CH_2Cl_2/hexane = 35/65 as an eluent. Compound **10** was obtained as a dark red solid (331 mg, 95%) and compound **11** as a dark greenish-blue solid (390 mg, 92%).

10: Mp = 221.5–224.8 °C, R_f = 0.40[c]. Compound **10** was identical to the compound described in the literature.[32,33] ^{1}H NMR (500 MHz, $CDCl_3$) δ 7.05 (s, 2H), 7.42–7.50 (overlapping multiplets, 12H), 8.04–8.08 (overlapping multiplets, 8H).

11: Mp = 183.5–187.0 °C, R_f = 0.24[d]. ESI-HRMS: *m*/*z*: 606.21601 $[M + H]^+$ ($C_{38}H_{26}BF_2N_3O_2$ + H^+ requires 606.21589 $[M + H]^+$). ^{1}H NMR (500 MHz, $CDCl_3$) δ 2.59 (s, 2H, C≡CH), 4.78 (d, J = 2.4 Hz, 2 × OCH_2), 6.94 (s, 2H), 7.08 (d, J = 7.1 Hz, 4H), 7.47–7.49 (overlapping multiplets, 6H), 8.02–8.07 (overlapping multiplets, 8H). ^{13}C NMR (125 MHz, $CDCl_3$) δ 159.3 (2 × C), 158.9 (2 × C), 145.5 (2 × C), 143.6 (2 × C), 131.8 (2 × C), 130.9 (4 × CH), 130.7 (2 × CH), 129.5 (4 × CH), 128.5 (4 × CH), 126.2 (2 × C), 117.8 (2 × CH), 115.2 (4 × CH), 78.3 and 75.9 (2 × C≡CH), 55.9(2 × OCH_2).

*4.1.2.5. Synthesis of **14**.* To a stirred solution of compound **11** (303 mg, 0.5 mmol) in dry toluene (10 mL), PPh_3 (26 mg, 0.1 mmol) and CuI (3.2 mg, 0.05 mmol) were added. The solution was treated with azido-PEG3-alcohol (175 mg, 1.0 mmol) and DIPEA (0.70 mL, 4 mmol). The solution was stirred under reflux for 2 h. After cooling to rt, the solvent was removed under reduced pressure and the residue was purified by flash chromatography with methanol/CH_2Cl_2 = 1/9 as an eluent. Compound **14** was obtained as a dark blue solid (239 mg, 50%).

14: Mp = 42.6–43.5 °C, R_f = 0.60[e]. ESI-HRMS: *m*/*z*: 978.39006 $[M + Na]^+$ ($C_{50}H_{52}BF_2N_9O_8$ + Na^+ requires 978.38922 [M +

Na]$^+$). ^{1}H NMR (500 MHz, DMSO-d$_6$) δ 3.37 (t, J = 5.2 Hz, 4H), 3.45–3.48 (overlapping multiplets, 8H), 3.51–3.53 (overlapping multiplets, 4H), 3.82 (t, J = 5.2 Hz, 4H), 4.54–4.57 (overlapping multiplets, 6H), 5.31 (s, 4H), 7.27 (d, J = 8.8 Hz, 4H), 7.47 (s, 2H), 7.55–7.57 (overlapping multiplets, 6H), 8.06–8.08 (overlapping multiplets, 4H), 8.19 (d, J = 8.8 Hz, 4H), 8.26 (s, 2H). ^{13}C NMR (125 MHz, CDCl$_3$) δ 159.7 (2 × C), 158.4 (2 × C), 144.6 (2 × C), 142.9 (2 × C), 142.2 (2 × C), 131.1 (2 × C), 130.9 (2 × CH), 130.7 (4 × CH), 129.3 (4 × CH), 128.5 (4 × CH), 125.0 (2 × C), 124.6 (2 × C), 118.4 (2 × CH), 115.2 (4 × CH), 72.2 (2 × CH$_2$), 69.5 (2 × CH$_2$), 69.4 (2 × CH$_2$), 68.6 (2 × CH$_2$), 61.2 (2 × CH$_2$), 60.1 (2 × CH$_2$), 49.3 (2 × CH$_2$).

*4.1.2.6. Synthesis of **15**.* To a stirred solution of compound **11** (300 mg, 0.5 mmol) in dry toluene (10 mL), PPh$_3$ (26 mg, 0.1 mmol) and CuI (3.2 mg, 0.05 mmol) were added. The solution was treated with benzyl azide (125 mg, 1.0 mmol) and DIPEA (0.70 mL, 4 mmol). The solution was stirred under reflux for 5 h. After cooling to rt, the solvent was removed under reduced pressure and the residue was purified by flash chromatography with ethyl acetate/CH$_2$Cl$_2$ = 1/9 as an eluent. Compound **15** was obtained as a reddish-dark blue solid (235 mg, 54%).

15: Mp = 220.2–223.8 °C, R_f = 0.69[f]. ESI-HRMS: m/z: 872.34405 [M + H]$^+$ ($C_{52}H_{40}BF_2N_9O_2$ + H$^+$ requires 872.34389 [M + H]$^+$). ^{1}H NMR (500 MHz, DMSO-d$_6$) δ 5.29 (s, 4H), 5.62 (s, 4H), 7.26 (d, J = 8.9 Hz, 4H), 7.31–7.38 (overlapping multiplets, 10H), 7.48 (s, 2H), 7.55–7.57 (overlapping multiplets, 6H), 8.07 (m, 4H), 8.19 (d, J = 8.9 Hz, 4H), 8.33 (s, 2H). ^{13}C NMR (125 MHz, CDCl$_3$) δ 159.6 (2 × C), 158.3 (2 × C), 144.5 (2 × C), 142.8 (2 × C), 142.6 (2 × C), 135.7 (2 × C), 131.0 (2 × C), 130.8 (2 × CH), 130.6 (4 × CH), 129.2 (4 × CH), 128.5 (4 × CH), 128.4 (4 × CH), 127.9 (2 × CH), 127.7 (4 × CH), 124.6 (2 × CH), 124.4 (2 × C), 118.3 (2 × CH), 115.1 (4 × CH), 61.2 (2 × CH$_2$), 52.7 (2 × CH$_2$).

4.2. Spectroscopic measurements

Dimethyl formamide (DMF; HPLC grade) was purchased from Merck (Darmstadt, Germany).

Absorption spectra were collected by employing a V730 UV-Vis spectrophotometer (Jasco, Tokyo, Japan). Fluorescence excitation and emission spectra were recorded using a Fluorolog τ3 spectrofluorometer (Jobin–Yvon/SPEX, Longjumeau, France). General spectroscopic properties of compounds **10**, **11**, **14**, and **15** were examined in 10 mm path-length quartz cuvettes, in DMF at room temperature.

4.3. Phototoxicity measurements

For the phototoxicity measurements, the A431 epidermoid carcinoma cell line (ATCC) was used. The cells were maintained in DMEM (Gibco, Thermo Fischer Scientific (Waltham, MA, US)) supplemented with 10% fetal calf serum, 2 mM L-glutamine, 100 U ml^{-1} penicillin, and 100 μg ml^{-1} streptomycin at 37 °C with 5% CO_2 and 95% humidity.

Compounds **10**, **11**, **14**, and **15** were dissolved in DMF (Sigma, Merck, Darmstadt, Germany) at a final concentration of 20 mM. For the irradiation procedure, 7.5 × 10^3 cells were seeded in 48-well plates (ThermoScientific) and incubated for 24 h. The next day, compounds **10**, **11**, **14**, and **15** with increasing concentrations (0–25 μM diluted in DMEM) were added to the cells and were incubated for another 24 h. Prior to illumination, the medium was removed from the cells and fresh DMEM (300 μl per well) was added. The plates were then irradiated from the bottom for 10 min (with periodical 30/15/30 s illumination) with a 658 nm LED light source (dose of 4 W cm^{-2}, in-house equipment). After illumination, the cells were incubated for 48 h at 37 °C with 5% CO_2 and 95% humidity before being assessed for cell viability. As a dark toxicity control, the experiments were performed under the same conditions but without illumination and keeping the plates in the dark throughout the experiment.

Cell viability was determined using PrestoBlue reagent (ThermoFisher Scientific, Waltham, MA, US) according to the manufacturers' instructions. Briefly, 5% PrestoBlue reagent diluted in phosphate-buffered saline (PBS) was added to the cells, and after 60 min incubation at 37 °C, fluorescence was measured in an Enspire fluorescent microplate reader (PerkinElmer, Waltham MA, US). The results are presented as the average of three independent biological replicates with three technical replicates in each experiment.

4.4. Measurement of ROS generation

The ROS generation potential of the dyes was measured using DCF-DA (2′,7′-dichlorofluorescein diacetate, Sigma, Merck, Darmstadt, Germany). 7.5 × 10^3 A431 cells were seeded on 48-well plates and incubated with compounds **10**, **11**, **14**, and **15** at 1–10 μM concentration. After 24 hours of incubation with **10**, **11**, **14**, and **15**, the cells were washed three times with PBS. Next, A431 cells were incubated with the cell-permeant DCF-DA dye (10 μM in HBSS) for 30 min at 37 °C with 5% CO_2 and 95% humidity, and then the cells were washed three times with PBS. Finally, the cells were illuminated for 10 min, as described in section 4.3, and fluorescence was measured in an Enspire fluorescent plate reader at 485/530 nm. The results are presented as the average of three independent biological replicates with three technical replicates in each experiment.

4.5. Statistical analysis

Statistical analysis was performed using Graph Prism v8.0.1 software (GraphPad Software Inc., San Diego, California). An unpaired t-test with Welch's correction was performed to compare the results with those of untreated samples. ns: $P > 0.05$; *: $P \leq 0.05$; **: $P \leq 0.01$; ***: $P \leq 0.001$.

Conflicts of interest

The authors declare that they have no known competing financial interests or personal relationships that could have appeared to influence the work reported in this paper.

Acknowledgements

This work was supported by the National Research, Development, and Innovation Office-NKFIH through projects OTKA SNN 139323, OTKA FK 128751, and OTKA K 138518. The help of Dr Krisztina Németh (Institute of Organic Chemistry, RCNS, Budapest) and Dr Péter Kele (Institute of Organic Chemistry, RCNS, Budapest) for providing the light source for illumination is greatly appreciated.

References

1 A. M. Smith, M. C. Mancini and S. Nie, Second window for *in vivo* imaging, *Nat. Nanotechnol.*, 2009, **4**, 710–711.
2 Y. Cai, Z. Wei, C. Song, C. Tang, W. Han and X. Dong, Optical nano-agents in the second near-infrared window for biomedical applications, *Chem. Soc. Rev.*, 2019, **48**, 22–37.
3 K. K. Ng and G. Zheng, Molecular Interactions in Organic Nanoparticles for Phototheranostic Applications, *Chem. Rev.*, 2015, **115**, 11012–11042.
4 X. Miao, W. Hu, T. He, H. Tao, Q. Wang, R.-F. Chen, L. Jin, H. Zhao, X. Lu, Q. Fan and W. Huang, Deciphering the intersystem crossing in near-infrared BODIPY photosensitizers for highly efficient photodynamic therapy, *Chem. Sci.*, 2019, **10**, 3096–3102.
5 T. Kowada, H. Maeda and K. Kikuchi, BODIPY-based probes for the fluorescence imaging of biomolecules in living cells, *Chem. Soc. Rev.*, 2015, **44**, 4953–4972.
6 J. Killoran, L. Allen, J. F. Gallagher, W. M. Gallagher and D. F. O'Shea, Synthesis of BF2 chelates of tetraarylazadipyrromethenes and evidence for their photodynamic therapeutic behaviour, *Chem. Commun.*, 2002, **17**, 1862–1863.
7 G. Grossi, M. Morgunova, S. Cheung, D. Scholz, E. Conroy, M. Terrile, A. Panarella, J. C. Simpson, W. M. Gallagher and D. F. O'Shea, Lysosome triggered near-infrared fluorescence imaging of cellular trafficking processes in real time, *Nat. Commun.*, 2016, **7**, 10855.
8 S. G. Awuah and Y. You, Boron dipyrromethene (BODIPY)-based photosensitizers for photodynamic therapy, *RSC Adv.*, 2012, **2**, 11169–11183.
9 A. Gorman, J. Killoran, C. O'Shea, T. Kenna, W. M. Gallagher and D. F. O'Shea, In Vitro Demonstration of the Heavy-Atom Effect for Photodynamic Therapy, *J. Am. Chem. Soc.*, 2004, **126**, 10619–10631.
10 N. Adarsh, R. R. Avirah and D. Ramaiah, Tuning Photosensitized Singlet Oxygen Generation Efficiency of Novel Aza-BODIPY Dyes, *Org. Lett.*, 2010, **12**, 5720–5723.
11 Q. Tang, W. Si, C. Huang, K. Ding, W. Huang, P. Chen, Q. Zhang and X. Dong, An aza-BODIPY photosensitizer for photoacoustic and photothermal imaging guided dual modal cancer phototherapy, *J. Matr. Chem.*, 2017, **5**, 1566–1573.
12 Y. Gawale, N. Adarsh, S. K. Kalva, J. Joseph, M. Pramanik, D. Ramaiah and N. Sekar, Carbazole-Linked Near-Infrared Aza-BODIPY Dyes as Triplet Sensitizers and Photoacoustic Contrast Agents for Deep-Tissue Imaging, *Chem. – Eur. J.*, 2017, **23**, 6570–6578.
13 H. Ş Çınar, Ş. Özçelik, K. Kaya, Ö. D Kutlu, A. Erdoğmuş and A. Gül, Synthesis and photophysical properties of monomeric and dimeric halogenated aza-BODIPYs, *J. Mol. Struct.*, 2020, **1200**, 127108–127117.
14 A. T. Byrne, A. E. O'Connor, M. Hall, J. Murtagh, K. O'Neill, K. M. Curran, K. Mongrain, J. A. Rousseau, R. Lecomte, S. McGee, J. J. Callanan, D. F. O'Shea and W. M. Gallagher, Vascular-targeted photodynamic therapy with BF2-chelated Tetraaryl-Azadipyrromethene agents: a multi-modality molecular imaging approach to therapeutic assessment, *Br. J. Cancer*, 2009, **101**, 1565–1573.
15 L. Ming and C. Li, Recent Advances in Activatable Organic Photosensitizers for Specific Photodynamic Therapy, *ChemPlusChem*, 2020, **85**, 948–957.
16 S. H. Lim, C. Thivierge, P. Nowak-Sliwinska, J. Han, H. Van Den Bergh, G. WagniHres, K. Burgess, H. B. Lee and J. Med, *Chem*, 2010, **53**, 2865–2874.
17 M. C. Malacarne, M. B. Gariboldi and E. Caruso, BODIPYs in PDT: A Journey through the Most Interesting Molecules Produced in the Last 10 Years, *Int. J. Mol. Sci.*, 2022, **23**, 10198–10220.
18 A. Kamkaew, S. H. Lim, H. B. Lee, L. V. Kiew, L. Y. Chung and K. Burgess, BODIPY dyes in photodynamic therapy, *Chem. Soc. Rev.*, 2013, **42**, 77–88.
19 J. F. Lovell, T. W. Liu, J. Chen and G. Zheng, Activatable photosensitizers for imaging and therapy, *Chem. Rev.*, 2010, **110**, 2839–2857.
20 X. Li, S. Kolemen, J. Yoon and E. U. Akkaya, Activatable Photosensitizers: Agents for Selective Photodynamic Therapy, *Adv. Funct. Mater.*, 2017, **27**, 1604053.
21 S. O. McDonnell, M. J. Hall, L. T. Allen, A. Byrne, W. M. Gallagher and D. F. O'Shea, Supramolecular photonic therapeutic agents, *J. Am. Chem. Soc.*, 2005, **127**, 16360–16361.
22 G. A. van Dongen, G. W. Visser and M. B. Vrouenraets, Photosensitizer-antibody conjugates for detection and therapy of cancer, *Adv. Drug Delivery Rev.*, 2004, **56**, 31–52.
23 J. Tian, J. Zhou, Z. Shen, L. Ding, J.-S. Yu and H. Ju, ApH-activatable and aniline-substituted photosensitizer for near-infrared cancer theranostics, *Chem. Sci.*, 2015, **6**, 5969–5977.
24 G. Fan, L. Yang and Z. Chen, Water-soluble BODIPY and aza-BODIPY dyes: synthetic progress and applications, *Front. Chem. Sci. Eng.*, 2014, **8**, 405–417.
25 J. Szabó, Z. Pataki, J. Wölfling, G. Schneider, N. Bózsity, R. Minorics, I. Zupkó and E. Mernyák, Synthesis and biological evaluation of 13α-estrone derivatives as potential antiproliferative agents, *Steroids*, 2016, **113**, 14–21.
26 Z. Shi, X. Han, W. Hu, H. Bai, B. Peng, L. Ji, Q. Fan, L. Li and W. Huang, Bioapplications of small molecule Aza-BODIPY: from rational structural design to in vivo investigations, *Chem. Soc. Rev.*, 2020, **49**, 7533–7567.

27 G. Yuan and D. F. O'Shea, Azadipyrromethenes: from traditional dye chemistry to leading edge applications, *Chem. Soc. Rev.*, 2016, **45**, 3846–3864.
28 J. T. Li, W. Z. Yang, S. X. Wang, S. H. Li and T. S. Li, Improved synthesis of chalcones under ultrasound irradiation, *Ultrason. Sonochem.*, 2002, **9**, 237–239.
29 C. A. M. Alonso, N. R. Candeias, D. P. Simão, A. F. Trindade, J. A. S. Coelho, B. Tan and R. Franzén, Comprehensive Organic Chemistry Experiments for the Laboratory Classroom, *RSC*, 2016, 951.
30 C. Niu, G. Li, A. Tuerxuntayi and H. A. Aisa, Synthesis and Bioactivity of New Chalcone Derivatives as Potential Tyrosinase Activator Based on the Click Chemistry, *Chin. J. Chem.*, 2015, **33**, 486–494.
31 G. Singh, J. Singh, S. S. Mangat and A. Aurora, Synthetic approach towards 'click' modified chalcone based organotriethoxysilanes; UV-Vis study, *RSC Adv.*, 2014, **4**, 60853–60865.
32 L. P. Jameson and S. V. Dzyuba, Aza-BODIPY: Improved synthesis and interaction with soluble Aβ1–42 oligomers, *Bioorg. Med. Chem. Lett.*, 2013, **23**, 1732–1735.
33 Y. Xu, M. Zhao, L. Zou, L. Wu, M. Xie, T. Yang, S. Liu, W. Huang and Q. Zhao, Highly Stable and Multifunctional Aza-BODIPY-Based Phototherapeutic Agent for Anticancer Treatment, *ACS Appl. Mater. Interfaces*, 2018, **10**, 44324–44335.